JOURNAL OF GEOPHYSICAL RESEARCH, VOL. 98, NO. E6, PAGES 10,941–10,949, JUNE 25, 1993

New Dust Opacity Mapping From Viking Infrared Thermal Mapper Data

TERRY Z. MARTIN

Jet Propulsion Laboratory, California Institute of Technology, Pasadena

MARK I. RICHARDSON[1]

Imperial College, London

Global dust opacity mapping for Mars has been carried forward using the approach described by Martin (1986) for Viking IR Thermal Mapper data. New maps are presented for the period from the beginning of Viking observations, until L_S 210° in 1979 (1.36 Mars years). This range includes the second and more extensive planet-encircling dust storm observed by Viking, known as storm 1977b. Improvements in approach result in greater time resolution and smaller noise than the earlier work. A strong local storm event filled the Hellas basin at L_S 170°, prior to the 1977a storm. Dust is retained in equatorial regions following the 1977b storm far longer than in mid-latitudes. Minor dust events appear to raise the opacity in northern high latitudes during northern spring. Additional mapping with high time resolution has been done for the periods of time near the major storm origins in order to search for clues to the mechanism of storm initiation. The first evidence of the start of the 1977b storm is pushed back to L_S 274.2°, preceding signs of the storm in images by about 15 hours.

INTRODUCTION

Mapping of dust opacity of the Mars atmosphere, using the silicate-induced absorption of 9 μm radiation, has been performed with the Viking Infrared Thermal Mapper (IRTM) data by *Hunt et al* [1980] for several local dust storms, and by *Martin* [1986] in a global sense. Martin, however, covered only the time period from areocentric solar longitude (L_S) 168° in 1976 to 270° in 1977, ending before the second and larger dust storm of 1977, known as storm1977b.

We present here first results from an effort to extend the earlier mapping work to the period of the 1977b major storm and beyond, and to concentrate attention on the details of opacity behavior during the initial phases of the 1977a and b storms. This work shows much additional information about the atmospheric behavior of Mars, offering the promise of interaction with currently developing models of global dynamics.

The opacity derivation process was described thoroughly by *Martin* [1986]. Briefly, the brightness temperature in the IRTM 6-8 μm band (T_7) is compared with that in the 8-10 μm band (T_9) to assess the depth of the silicate band produced by airborne dust. That depth is modeled, using a delta-Eddington radiative transfer code and a model atmosphere derived from knowledge of the temperature at the 0.6 mbar level (T_{15}) and assumptions about the behavior of the temperature profile near the surface under normal midday conditions. The opacity is varied until the value of modeled $T_7 - T_9$ compares favorably with the actual value. It is important to note that the opacities derived here refer to a wavelength of 9 μm; by comparison with Viking Lander opacities, we found that visible band opacities are typically a factor of 2.5 larger [*Martin*, 1986].

In the process of gearing up to extend the earlier effort, certain improvements were explored that enhanced the quality of these maps. First, we studied the effect of altering the size of the time period for each map. In the earlier work the seasonal bin size was 10°. The Mars atmosphere undergoes changes on much shorter time scales during dust storms. However, the Viking orbiters, even in time periods when their orbits "walked" around the planet, took weeks to cover all longitudes. In a partial attempt to get better time resolution, a bin size of 5° was chosen for the new work. The coverage in any single map will be less than for a 10° map. Still, it is evident that we are not doing justice to the short time scales of change during dusty periods.

Second, we developed a better way to remove the effect of local variations of temperature upon the derived opacity. Within a single latitude/longitude bin, it is possible for uneven sampling by the 7 and 9 μm channels to produce undesirable $T_7 - T_9$ differences due to the diurnal change of temperature, albedo and inertia contrasts, slopes, etc. We had in earlier work removed these effects by subtracting a model temperature for each measured spot, prior to forming the difference $T_7 - T_9$ for one latitude/longitude bin:

$$(T_7 - T_9)_{bin} = \frac{1}{R}\sum_{i}^{R}(T_{7i} - T_{Mi}) - \frac{1}{S}\sum_{j}^{S}(T_{9j} - T_{Mj})$$

where T_{7i} is the individual T_7 measurement in a bin, likewise for T_9, and T_{Mi} and T_{Mj} are the model values at the measurement locations. We found, however, that subtracting the value of T_{20} (brightness temperature in the 18-24 μm band), which is

[1]Now at Dept. of Earth and Space Sciences, University of California, Los Angeles.

Paper number 93JE01044.
0148-0227/93/93JE-01044$05.00

available for each point, is far preferable, since T_{20} responds to exactly the effects we are trying to remove, whereas the model represents only diurnal and latitudinal effects. This change has greatly reduced the apparent spatial "noise" in the opacity maps.

Third, we have used more conservative constraints on the input data. In the earlier work, negative lapse rates were allowed (T_{15} values exceeding surface temperatures), since the opacity routine in principle works as well with a monotonic negative rate as with a normal positive one. Many of the very high opacities derived earlier in the southern polar regions were found to be associated with negative lapse rate conditions. Since we do not have information about the details of the temperature profile, or where the bulk of the dust resides, and since models are less reliable for these polar dusty situations, we chose to disallow opacity calculation for the negative lapse rates.

It should be noted that isothermal and negative lapse rate conditions are possible under very high dust loading, and perhaps in the downwelling region of a dust-driven Hadley circulation [*Haberle et al.*, 1982; *Pollack et al.*, 1990]. *Lindal et al.* [1979] showed evidence of this behavior in radio occultation profiles at latitude +38° at L_S 297°, when dust from the 1977b storm was still abundant. The bias introduced by ignoring these special lapse rate conditions must be assessed. We therefore explored whether unusual combinations of the T_7, T_9, and T_{15} values collected for this work were occurring during high opacity time periods. As expected, the bulk of such occurrences is found near the south polar cap edge. In some cases the value of T_9 exceeds both T_7 and T_{15}, indicating a temperature maximum above the surface, but at a level in the atmosphere below that sampled by T_{15} (about 23 km). Such cases are likely where the surface is constrained to be cold, and the atmosphere above it warms up.

Of greater interest are several cases found in a few nonpolar areas during the 1977a-b storm period. These occurrences are represented in Table 1. For the 1977a storm, only one latitude/longitude bin in each map is affected in the region just north of our map coverage for L_S 215-225°, well after the inception of that dust event. For the 1977b storm, a larger area (about nine bins) is affected in southern equatorial latitudes during L_S 275-280° just after the beginning of that storm. Later, a substantial longitude zone (about 26 bins) is affected to the east of the VL-1 site during L_S 285-290°. Finally, it is noteworthy that the example in one bin at L_S 295-300° corresponds well to the inversion found by Lindal at the same latitude and season. Although these cases imply by their unusual thermal behavior the presence of substantial dust in the atmosphere, they are somewhat localized, and not very common. They represent a small fraction of the area covered in the affected maps.

THE 5° OPACITY MAP SET

The set of maps produced with the 5° L_S bin size is presented in Plate 1. Each map shows opacity for a 5° L_S period; the starting L_S value is shown beneath, for every other period. Coverage is pole to pole; 0° longitude is at the right side; an elevation map at the same resolution is shown for reference in Figure 1. This set covers the time period from the arrival at Mars of the Viking Orbiter 1, at L_S 84° in 1976, to the end of effective coverage by VO1 in 1979 at L_S 210°. Viking Orbiter 2 arrived later than 1 (L_S 105°) and ceased operation earlier, at L_S 118° in 1978. VO2 had a higher inclination orbit and provided better data than VO1 at high latitudes. Early mission spatial coverage is very limited because the orbiters were engaged primarily in selection of landing sites at a narrow range of latitudes. There is a gap in coverage between L_S 150 and 168° in 1976 due to solar conjunction. At the end of the VO1 mission, global mapping was not being done, and coverage deteriorates to narrow strips.

The major features of these maps are the two planet-encircling dust storms of 1977, both occurring during the nominal dust storm "season" defined by the period when storms have been observed telescopically. Viking was fortunate to observe these storms; statistically, it has become evident that storms such as those seen by Mariner 9 and Viking are not common [*Zurek and Martin*, 1993].

Of additional interest, and described here for the first time, are other dust events taking place at times outside the dust storm season or leading up to it. Such phenomena provide unique evidence of dynamic conditions conducive to dust raising, and therefore offer valuable constraints to models of Martian atmospheric dynamics.

We discuss now details of the opacity maps (Plate 1). The early Viking mission was characterized as a period of low dust opacity, and that is certainly the case relative to the storm-dominated period in 1977. However, the planet does not not show uniformity during northern summer. There is evidence of local storm activity, indicated by opacities greater than about

TABLE 1. Instances of Near-Isothermal Conditions (Typical)

L_S	Latitude	Longitude	T_7	T_9	T_{15}	Hour
215-220	44 to 48	270-276	204	200	200	12.0
220-225	44 to 48	264-270	208	207	209	12.0
275-280	-24 to -12	78-96	230	232	214	12.0
280-285	-64 to -60*	48-54	223	224	226	4.0
285-290	20 to 32	258-30	213	214	213	10.7
295-300	36 to 40	72-78	206	208	208	11.0

*Typical polar example.

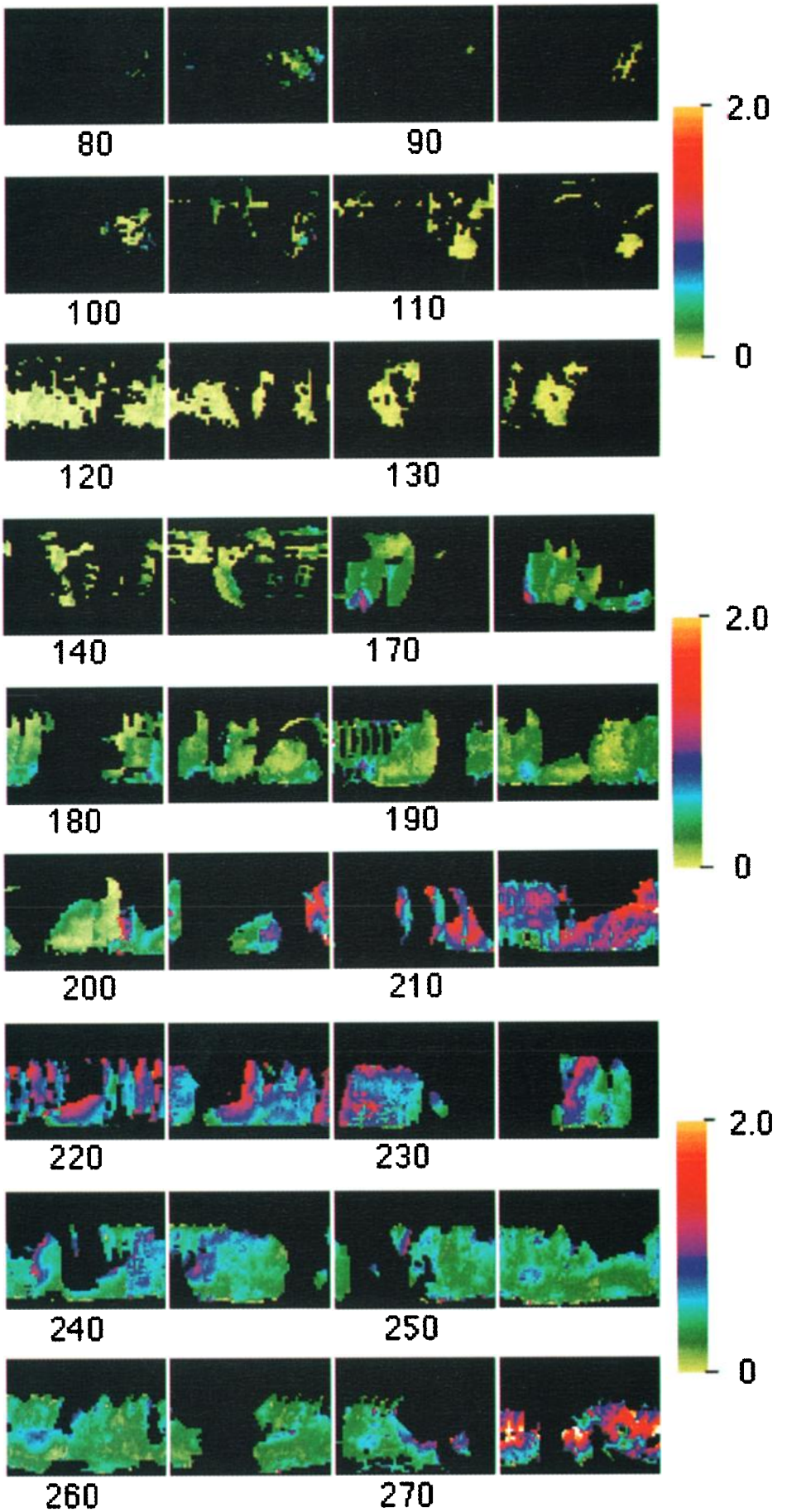

Plate 1. Global maps of 9 μm dust opacity for 5° L_s bin size. For each map, the North Pole is at the top, south at the bottom. Longitude 0° is at the right side, and 360° at the left (see Figure 1). The starting L_s value is shown for every other bin. Black indicates lack of coverage. The color scale covers the opacity range from 0 to 2.0; values above 2.0 are shown at the maximum level (white).

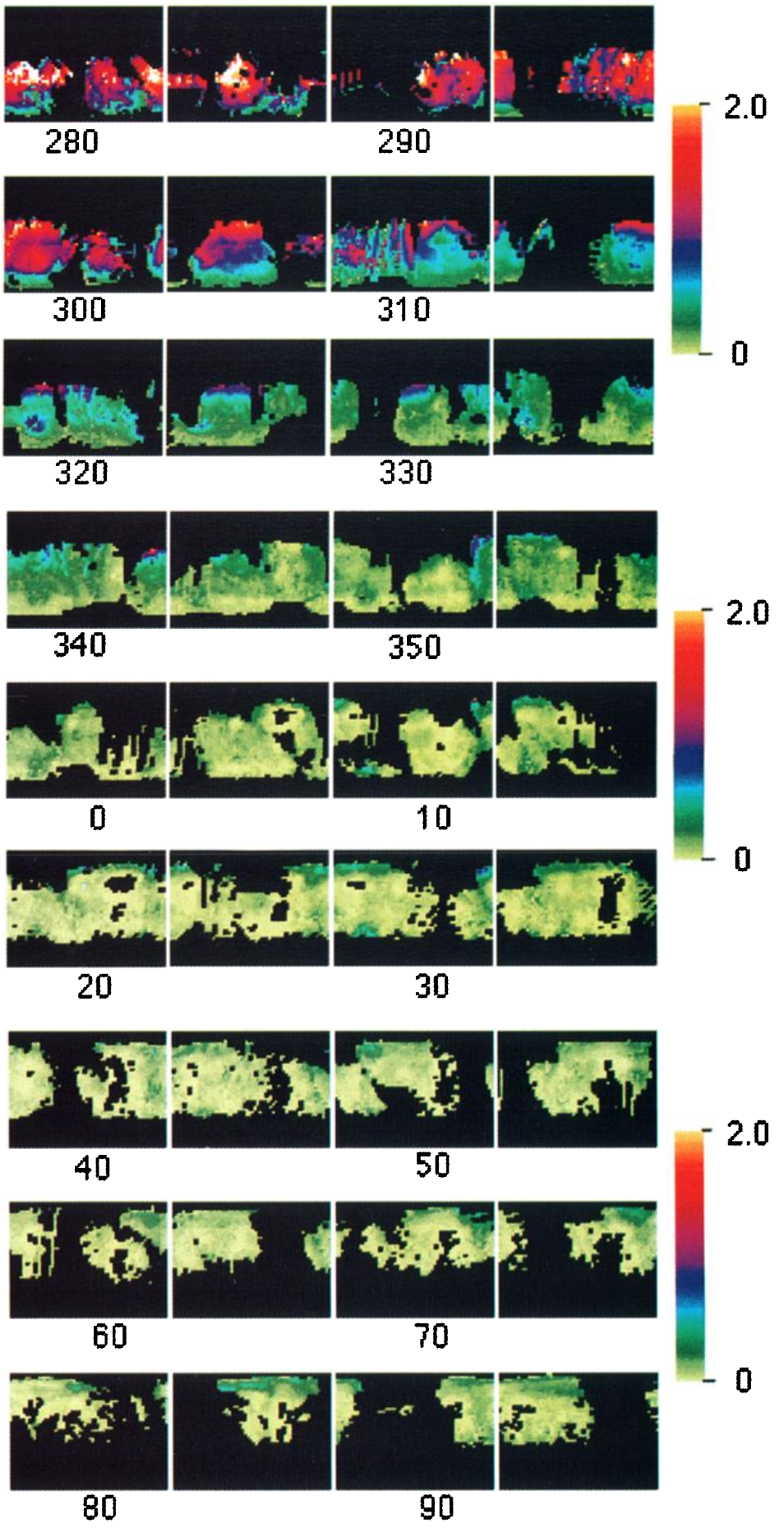

Plate 1. (continued)

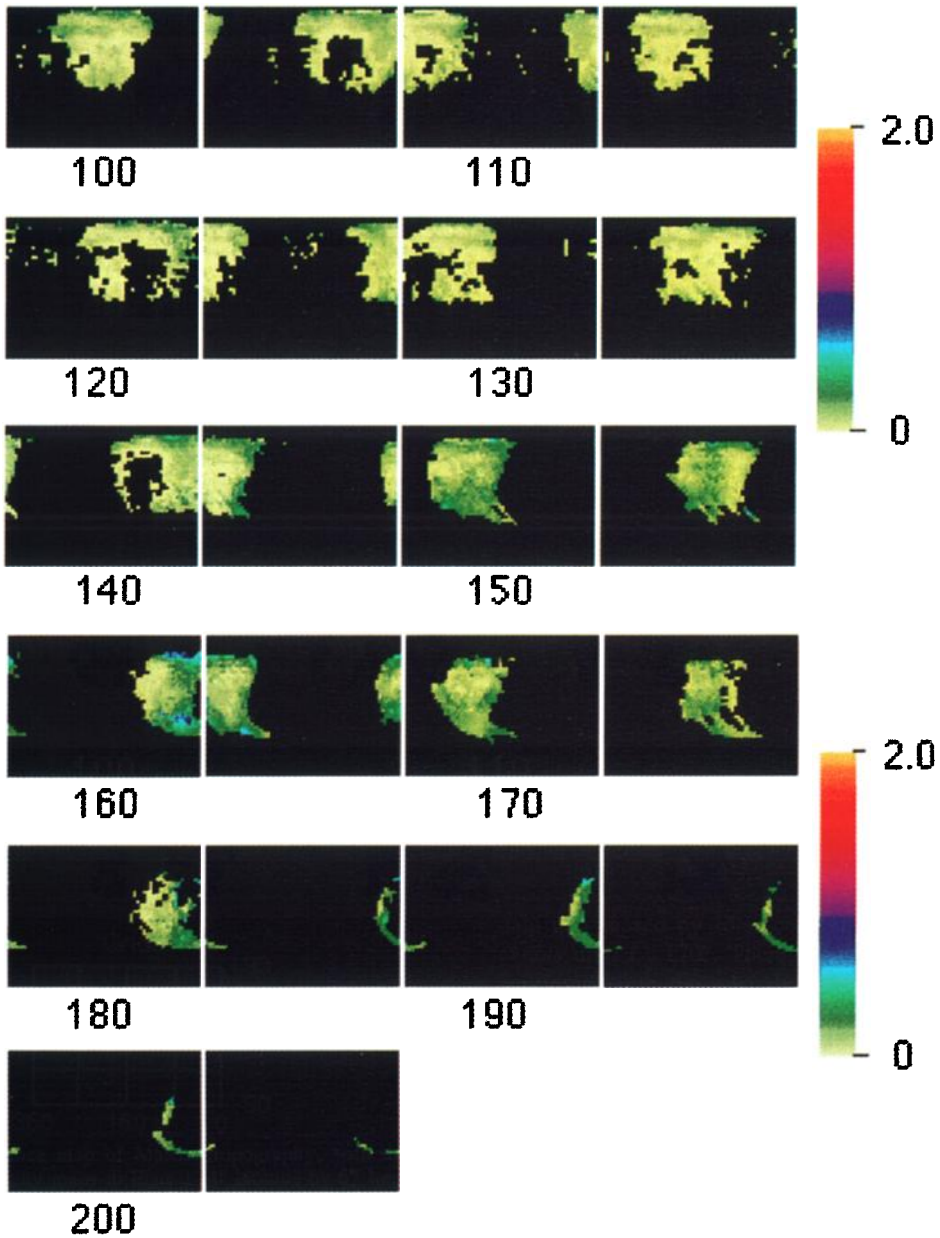

Plate 1. (continued)

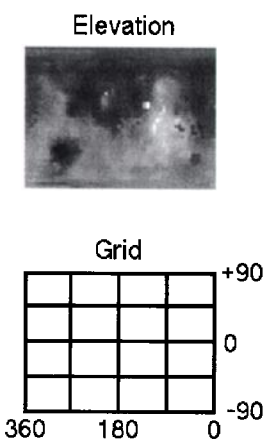

Fig. 1. (Top) Reference map of Martian topography, with the same resolution as the opacity maps in Plate 1 (4° latitude by 6° longitude). Elevations range from about -3 km in Hellas (dark, lower left) to about +25 km at the summits of volcanoes on the Tharsis uplift (center right). (Bottom) Reference grid of latitude/longitude for superposing on the opacity maps.

0.5 at 9 μm, in several equatorial regions between L_S 85 and 110°. The VL-1 site is not included in this activity, which concentrates to the south and east. Additional activity may of course be present in regions not covered.

There is little change of note after L_S 110° until 145°; then, we begin to see more evidence of locally higher opacity both in high northern latitudes and in the south. Unfortunately, the data gap caused by solar conjunction keeps us from tracking events until L_S 170°. There, we find a major event in Hellas, continuing into the next time period. Argyre is also seen to have dust activity distinct from its surroundings during L_S 175-185°.

The general level of opacity builds steadily after about L_S 145°, as was noted in the VL-1 opacity record [*Colburn et al.*, 1989]. Hellas is again prominent from L_S 185° to 200°. Some of that visibility is due of course simply to the greater path to the surface; Hellas is up to 3 km lower than its surroundings, which would imply 35% greater opacity if the dust follows a 10-km scale height. During the L_S 200-205° frame, we see the beginning of the 1977a storm (see below for details). The

strong opacity contrast near longitude 90° is due to the imperfect sampling in time and space; data to the left were acquired early in the period, and to the right, near the end. The continuation of this spatial coverage can be seen, as the storm progresses, in the center of the L_S 205-210° frame.

The storm itself makes evident the inadequacy of the Viking sampling. Even though the infrared data covered much greater areas than the imaging data, the progression of the event is undersampled. The incoherence between successive days' coverage is readily seen in the L_S 220-225° frame. One of the curious features at L_S 215° is that Hellas appears as a region of lower opacity than its surroundings, as if it were isolated from the global behavior. Possibly the event earlier at L_S 170° there depleted Hellas as a source region. Alternatively, regional winds may have abated so that dust raising ceased. The phenomenon is not due to lack of thermal contrast in that area. Notice that Hellas remains at low opacity in successive frames, until L_S 230°.

Several general conclusions about the 1977a storm may be drawn from these new maps. It is apparent that the latitudinal extent of the storm is large; equatorial and northerly regions to the limit of our coverage (about +40°) are involved. Second, there is evidence of a particularly active part of the storm in a broad area centered near the equator at longitude 220°; compare the three frames beginning with L_S 215°. The opacity lingers at high values primarily in the hemisphere west of 180° after L_S 245°.

The 1977b storm inception is described below. Although its details are again in some doubt because of the sampling problem, certain effects can be reliably shown. The highest opacity values, well above 2.0 (saturated in our representation) occur near the equator. Latitudes poleward of about -60° do not seem involved in the storm to any significant degree. Even the highest elevation region, Tharsis, experiences opacities above 1.5; although Tharsis commonly is distinguished in this map set by low opacities (see L_S 5-80°), it is not distinct during the 1977b storm.

The lack of involvement of southerly polar regions in the 1977b storm is in disagreement with recent modelling by *Murphy and Leovy* [1991] of the time variation of opacity following insertion of dust at southern midlatitudes.

An interesting pattern emerges as the dust settles. Southerly latitudes have largely reverted by L_S 315° to values below 0.5. However, high opacities linger north of the equator, at the limit of our coverage. Opacity near 1.0 is found even at L_S 350-355°. This pattern is reminiscent of that described by *Anderson and Leovy* [1978] for the great storm observed by Mariner 9 in 1971-1972. Their conclusion, also applicable here, is that the diurnal atmospheric tide [*Zurek*, 1976] is reponsible for sustained mixing of dust in equatorial regions during the decay phase of global dust storms.

After the last effects of the 1977b storm have abated, the planet enters a long period of relative quiet, which however has consistent phenomena present. The elevation map of the planet plays a controlling role, with Hellas and Tharsis usually distinct. Equatorial opacities fall to mean levels about 0.1. Between L_S 10 and 40°, increased dustiness above latitude +45° signifies the presence of local storms there. A site of particular activity is Acidalium (+50, 30°), although many longitudes show the effect.

Moving into the second Mars year, we find a continuation of the activity in northern latitudes. The high surface temperatures at the beginning of northern summer are likely responsible, through convective phenomena such as dust devils [*Ryan and Lucich*, 1983; *Thomas and Gierasch*, 1985], for the evidence of airborne dust. There is little to distinguish the opacity behavior compared between the first and second year. The first year has a few local high dust indications prior to L_S 110°; the second year shows none in equatorial regions. Between L_S 110° and 150°, there is no important difference in global opacity levels. However, the significant increase in overall levels for year 1 that occurred during the (unobserved) solar conjunction period did not seem to happen in year 2 (Figure 2).

Towards the end of coverage, there is in year 2 no indication of the presence of a dust storm like 1977a; this finding is consistent with the Viking Lander opacity record. It may be that the opacity levels necessary for dust storm initiation [*Leovy et al.*, 1973] are higher than those present at L_S 200° in year 2.

There has arisen recently new evidence that the low-opacity periods observed by Viking are not indicative of how clear the atmosphere can become. Temperature profiles derived from Earth-based microwave observations [*Clancy et al.*, 1990] show atmospheric temperatures well below those obtained with the IRTM 15-μm band (presented by *Martin* [1981]). Atmospheric temperature at the level sampled, about 0.6 mbar, is sensitive to the dust present. Thus, the low opacities that dominate in our Viking data set for long periods (see histogram in *Martin* [1986]) may not be representative of the clearest state attainable by the Martian atmosphere.

ORIGINS OF MAJOR DUST STORMS

As a secondary task, we undertook the detailed investigation of opacity behavior near the origin of the two major dust storms of 1977. A description of the imaging experiment data relating to these two events was given by *Briggs et al.* [1979]. Those data were also used quantitatively by *Thorpe* [1979] in deriving visual opacity histories. Meteorological evidence at the two Viking Lander stations for the storms was described by *Ryan and Henry* [1979], complementing the Lander imaging opacity data described by *Pollack et al.* [1977, 1979] and by *Colburn et al.* [1989]. *Martin* [1986] described IRTM opacity data for those two sites. Although the IRTM data are typically more thorough in coverage than those of the imaging experiment, no detailed description of the storms' inception has yet been given from the global IRTM point of view.

We isolated the set of IRTM observations obtained in the relevant time periods, and then grouped several sequences that occurred within about 2 hours in order to form a set of "frames." The set of these frames (Plate 2) is not uniformly spaced, and some of the gaps are larger than is desirable. However, certain conclusions of value can be drawn.

For the 1977a storm, there is no evidence in the IRTM data for opacities above about 0.6 until L_S 206.4° (the fourth frame), at which point the storm is very plainly seen, already with a spatial extent of about 90° in longitude, and a latitudinal extent from the equator to the southern edge of coverage near -60°. The storm extent is roughly comparable to that described by *Thorpe* [1979] in his tracking of the expansion of the 1977a event. There is unfortunately a gap of 4.3° in L_S between this frame and the previous one (about 7 Mars days) during which time the storm has evidently been initiated. The first note of the storm in imaging data was at L_S 205.6°, 30 hours prior to our frame four. It was seen in Thaumasia Fossae,

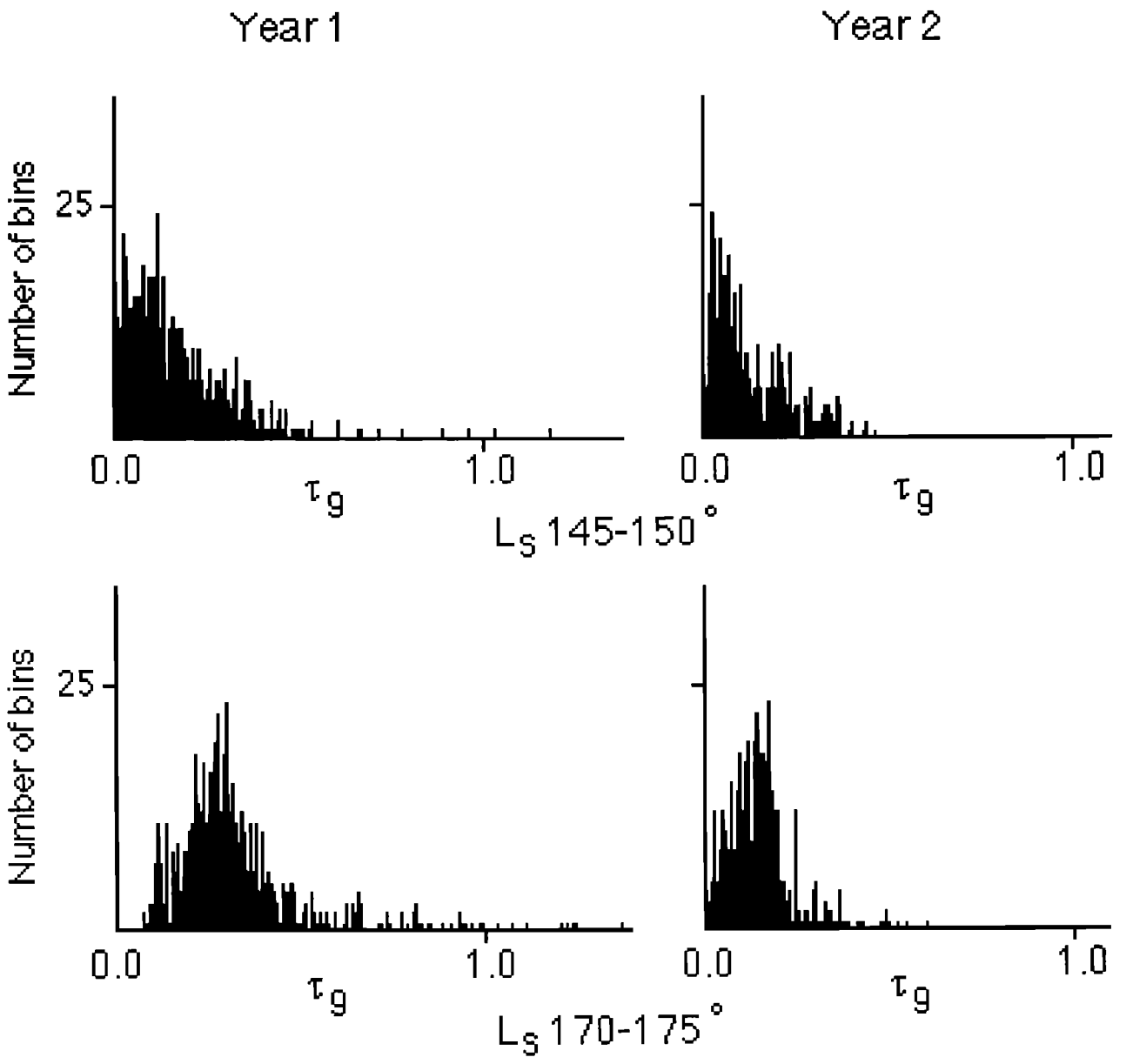

Fig. 2. Comparison of opacity histograms between Mars year 1 (left pair) and year 2. Data are taken from opacity maps having good spatial coverage. Axes are number of bins versus 9-μm dust opacity. Opacity levels are comparable for L_S 145-150° (top pair) for both years. During L_S 170-175° (bottom pair) there was a substantial increase in year 1, but not in year 2.

roughly -40°, 90° in latitude/longitude space. That location is well within the boundaries of the storm in our frame four; fortunately, our coverage is broad enough to locate the edge of the storm at that time. If we assume there was only one storm origin, then the next frame, at L_S 207.4°, shows movement towards 0° longitude, the only region where we have coverage then. The storm has spread at least to about +10° and to 0° longitude at -50°. The last frame of this set, at L_S 208.0°, shows opacities well above 1.0 into northern midlatitudes, including the VL-1 site.

The 1977b storm is covered in the IRTM data by both Viking Orbiter 1 and 2 data (Plate 2). At L_S 272.6°, there is evidence of local storm activity in Isidis Planitia and to the south. Our next frame, at 274.1°, shows additional storm activity with opacities between 0.8 and 1.2 in a range of southern highland regions from about longitude 150 to 230°. The eastern edge of the activity cannot be defined in this frame. The timing of our L_S 274.1° frame is of interest because it precedes by about 15 hours the first evidence in imaging data for this storm (VO-2 revolution 287, L_S 274.5°; *Briggs et al.* [1979]).

The next frame, at L_S 279.3°, is too much later to be of value in locating the storm origin. At this point all longitudes appear to be involved, with opacities exceeding 2.0 over wide areas. Latitudes below -50°, however, show only slight change. It appears likely that the storm spread more effectively to equatorial regions than to the south.

Thorpe [1979] provided a sequence of opacity maps for the 1977b storm based on imaging data. Unfortunately, the IRTM coverage of low longitudes is meager until well after the storm spreads out, so that we cannot verify the origin being near

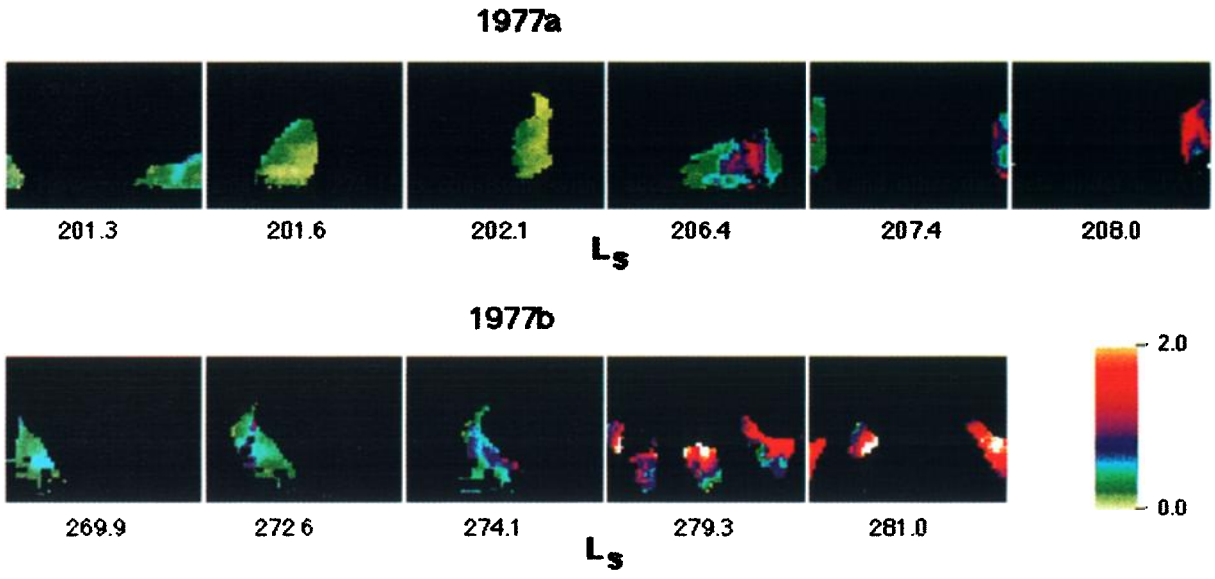

Plate 2. Global maps of 9-μm dust opacity for observation sequences near the start of the 1977a and 1977b dust storms. For each map, the North Pole is at the top, south at the bottom. Longitude 0° is at the right side, and 360° at the left. Black indicates lack of coverage. The color scale covers the opacity range from 0 to 2.0; values above 2.0 are shown at the maximum level (white).

Argyre. However, our frame at L_S 274.1° is consistent with Thorpe's L_S 274° figure showing a peak dust concentration between -40 to -50° latitude, expanding to the west and north with time.

The overall impression of the Viking era major storms 1977a and 1977b is that they bear strong resemblance to the storms that have been observed telescopically [e.g., *Martin*, 1974*a*,*b*; 1976]. Storm growth initiates in southern middle latitudes, progresses most rapidly to the east and west, and more slowly north and south, with dissipation occurring in some cases before the northern hemisphere is greatly affected. The Viking Landers did not characterize the full opacity magnitude of either storm.

Conclusions

This new set of opacity maps makes possible a range of intercomparisons with theoretical studies of Martian atmosphere dynamics. It is evident that complete information on the spatial evolution of storms and a characterization of the vertical distribution of dust and the wind fields are lacking in these maps, constraining the extent of model comparisons that can be done. However, global circulation models (GCM's) that incorporate dust now have available constraints upon the thermal and opacity conditions that exist prior to major storm events, the latitudinal distribution of dust after storm initiation, and the character of dust fallout. Additional work may be possible in modeling northern local storm behavior. The interannual variability of dust storms can be studied given the year 2 behavior. Finally, opacity histories for specific sites on the planet can be developed, as an aid to the study of dust transport.

Acknowledgments. This work takes advantage of software developed at the Planetary Data System Radiometry Node (U.S. Geological Survey, Flagstaff) by H.H. Kieffer and R. Gurule to treat radiometry data sets. That system, known as XG, allows access to the IRTM and other data sets under a TAE-driven interface operating on VAX VMS systems. Another PDS-developed item, the compact disk (CD-ROM) version of the IRTM data, permitted ready access to the data set. M. Richardson participated in this work as a 1991 Summer Undergraduate Research Fellow at the California Institute of Technology. The research described in this paper was carried out by the Jet Propulsion Laboratory, California Institute of Technology, under a contract with the National Aeronautics and Space Administration.

References

Anderson, E., and C. Leovy, Mariner 9 television limb observations of dust and ice hazes on Mars, *J. Atmos. Sci.*, *35*, 723, 1978.

Briggs, G.A., W.A. Baum, and J. Barnes, Viking Orbiter imaging observations of dust in the martian atmosphere, *J. Geophys. Res.*, *84*, 2795, 1979.

Clancy, R.T., D.O. Muhleman and G.L. Berge, *J. Geopys. Res.*, *95*, 14,543-14,554, 1990.

Colburn, D. S., J. B. Pollack, and R. M. Haberle, Diurnal variations in optical depth at Mars, *Icarus*, *79*, 159, 1989.

Haberle, R.M., C.B. Leovy, and J.B. Pollack, Some effects of global dust storms on the atmospheric circulation of Mars, *Icarus*, *50*, 322, 1982.

Hunt, G.E., E.A. Mitchell, and A.R. Peterfreund, The opacity of some local Martian dust storms observed by the Viking IRTM, *Icarus*, *41*, 389, 1980.

Leovy, C.B., R.W. Zurek, and J.B. Pollack, Mechanisms for Mars dust storms, *J. Atmos. Sci.*, *30*, 749, 1973.

Lindal, G.F., H.B. Hotz, D.N. Sweetnam, Z. Shippony, J.P. Brenkle, G.V. Harsell, R.T. Spear, and W.H. Michael, Jr., Viking radio occultation measurements of the atmosphere and topography of Mars: Data acquired during 1 Martian year of tracking, *J. Geophys. Res.*, *84*, 8443-8456, 1979.

Martin, L.J., The major Martian yellow storm of 1971, *Icarus*, *22*, 175, 1974*a*.

Martin, L.J., The major Martian dust storms of 1971 and 1973, *Icarus*, *23*, 108, 1974*b*.

Martin, L.J., 1973 dust storm on Mars: Maps from hourly photographs, *Icarus*, *29*, 363, 1976.

Martin, T.Z., Mean thermal and albedo behavior of the Mars surface and atmosphere over a Martian year, *Icarus*, *45*, 427, 1981.

Martin, T.Z., Thermal infrared opacity of the Mars atmosphere, *Icarus, 66*, 2, 1986.

Murphy, J. R., and C.B. Leovy, Mars dust storm simulations: Analysis of surface stress, paper presented at Workshop on Martian Surface and Atmosphere Through Time, Lunar and Planet. Inst., Boulder, Colo., Sept. 23-25, 1991.

Pollack, J.B., D. Colburn, R. Kahn, J. Hunter, W. Van Camp, C. Carlston, and M. Wolfe, Properties of aerosols in the Martian atmosphere, as inferred from Viking Lander imaging data, *J. Geophys. Res., 82*, 4479, 1977.

Pollack, J.B., D. Colburn, F.M. Flasar, R. Kahn, C. Carlston, and D. Pidek, Properties and effects of dust particles suspended in the Martian atmosphere, *J. Geophys. Res., 84*, 2929, 1979.

Pollack, J.B., R.M. Haberle, J. Schaeffer, and H. Lee, Simulations of the general circulation of the Martian atmosphere, 1, Polar processes, *J. Geophys. Res., 95*, 1447, 1990.

Ryan, J.A., and R.M. Henry, Mars atmospheric phenomena during major dust storms, as measured at surface, *J. Geophys. Res., 84*, 2821, 1979.

Ryan, J.A., and R.D. Lucich, Possible dust devils, vortices on Mars, *J. Geophys. Res., 88*, 11,005, 1983.

Thomas, P.C., and P.J. Gierasch, Dust devils on Mars, *Science, 230*, 175, 1985.

Thorpe, T. E., A history of Mars atmospheric opacity in the southern hemisphere during the Viking extended mission, *J. Geophys. Res., 84*, 6663, 1979.

Zurek, R.W., Diurnal tide in the martian atmosphere, *J. Atmos. Sci., 33*, 321, 1976.

Zurek, R.W., and L.J. Martin, Interannual variability of planet-encircling dust storms on Mars, *J. Geophys. Res., 98*, 3247, 1993.

T.Z. Martin, Mail stop 169-237, Jet Propulsion Laboratory, 4800 Oak Grove Drive, Pasadena, CA 91109.

M.I. Richardson, Dept. of Earth and Space Sciences, University of California, Los Angeles, CA 90024.

(Received January 30,1993;
revised March 1993;
accepted April 16, 1993.)